Table 2 TCRVA and TCRVB usage of BC clones

BC clone	TCRVA	TCRVB
20.7	(AV25S1)FCAGHNAG(AJ14S3)	(BV12S3)CASRQAGTAYE(BJ2S7)
33.5	(AV3S1)FCATERGQ(AJ13S2)	(BV6S1A1)CASSPTGTANT(BJ1S1)
42.1	(AV8S1A1)FCAASLDNY(AJ126)	(BV5S1A1)CASRRSTGE(BJ2S2)

TCRVA and VB usage are shown, with amino acid sequences in the N(D)N region.

TGG ATT TAG AGT CTC TC), respectively. A panel of labeled TCRAV-specific oligonucleotide probes (Table 1) were used to study TCRAV gene usage with PCR-ELISA.[10] First, seven pools of the AV-specific probes were hybridized with immobilized PCR products in microplates to find out positive wells. Then, the products were hybridized with individual AV probes in another set of plates to pin-point the AV genes predominantly used by the cDNA. To clone the entire variable region cDNA, cDNA were amplified with CA4 and reamplified with a nested primer, CA2 (5'-ACG CGT CGA CAC TGG ATT TAG AGT CTC TC). The products were subcloned into pBluscript II SK+ (Stratagene, La Jolla), and recombinant clones with the dominant VA gene were selected with dot blot DNA hybridization using corresponding VA-specific oligonucleotides. After sequence determination of these clones, dominant clones were selected as cDNA for the T cell clones.

RESULTS

TCRVA AND VB SEQUENCES

TCRVA and VB sequences of three T-cell clones BC 20.7, BC33.5 and BC42.1 are shown in Table 2. The N (D)N region sequences are shown as one-letter codes for amino acids, between V and J segments in parentheses. As described in our earlier studies, these T-cell clones recognize BCGa p84-100 (EEYLILSARDVLAVVSK; with first anchor underlined), in the context of HLA-DRB1*1405.[4] It is especially important to note that N(D)N region consists of 8 and 11 residues at TCRVA and VB of BC20.7 and BC33.5, respectively, whereas that of BC42.1 consists of 9 and 9 residues, repectively.

STIMULATORY ACTIVITIES OF BCGA P84-100-DERIVED ANALOG PEPTIDE L87V TO BC20.7

To evaluate the effects of single amino acid substitutions, proliferation and lymphokine production in response to analogue peptides were determined and findings were compared with those seen with the wild-type peptide. Most of the analogue peptides that stimulated BC clones showed a pattern of lymphokine production similar to that for the wild-type peptide (not shown). However, IFN-γ production of BC20.7 was increased in response to several analogue peptides at high concentration (16 μM), especially peptide L87V in which Leu is replaced by Val at the 87 th residue of the peptide BCGa p 84-100, whereas neither T cell proliferation nor production of other lymphokines, showed any remarkable change ; *i.e.*, only the production of IFN-γ was affected for recognition of the analog peptide L87V. As shown in Figure 1, to determine whether or not the change of IFN-γ production was due to differences in the HLA-peptide or TCR-TCR ligand avidity between L87V and the wild-type peptide, responses of BC20.7 to several different concentrations of L87V were compared with those of the wild-type peptide. In the range of concentrations from 0.016 μM up to 16 μM, IFN-γ production in response to L87V constantly exceeded that of the wild-type peptide. Moreover, the plateau level of L87 V-driven IFN-γ production was significantly higher. Mean IFN-γ production of BC20.7 for L87V increased significantly in comparison to the wild-type, whereas no statistical differences were noted in proliferative responses between R21K and the wild-type at a range of 0.16 μM to 16 μM. The IL-4 production of BC20.7 for each analogue peptide was proportional to the proliferative response to each peptide, at a range of 0.0016 to 16 μM (not shown). In contrast, production of GM-CSF gradually increased, in a dose-dependent manner throughout the range of 0.016 to 16 μM. These data indicate that the plateau responses and proliferation of IFN-γ are not due to saturation of the TCR ligand on the APC surface.

STIMULATORY ACTIVITIES OF BCGA P84-100-DERIVED ANALOGUES TO THREE BC CLONES

All three T-cell clones were stimulated with analogues at 16 μM, with replacements at P1 (=86Y) through P9 (=94V). Table 3 summarizes the results, regarding proliferative responses and IFN-γ production. P1 (=86Y) replaced by Ala (A) indicates a peptide species EEALILSARDVLAVVSK. Relative IFN-γ responses are shown, where IFN-γ production was divided by proliferation. P1 replaced by A gave values of 96/100/98, indicating that BC20.7,BC33.5 and BC 42.1 exhibited 96%, 100% and 98% responses respectively, as compared with the wild-type. Asterisks indicate peptide species that did not exert full agonistic activity ; *i.e.*, peptide stimulation even at 16 μM did not give a plateau response.

Most of analogues that exhibited full agonistic activity, stimulated IFN-γ production at levels roughly similar to the wild-type peptide, *i.e.*, at around 100%. However, it is important to note that L87T,L87S,L87A, and L87V significantly($p<0.01$) induced increased levels of IFN-γ production of BC20.7 and BC33.5, but not of BC42.1. Such a clone-specific phenomenon was

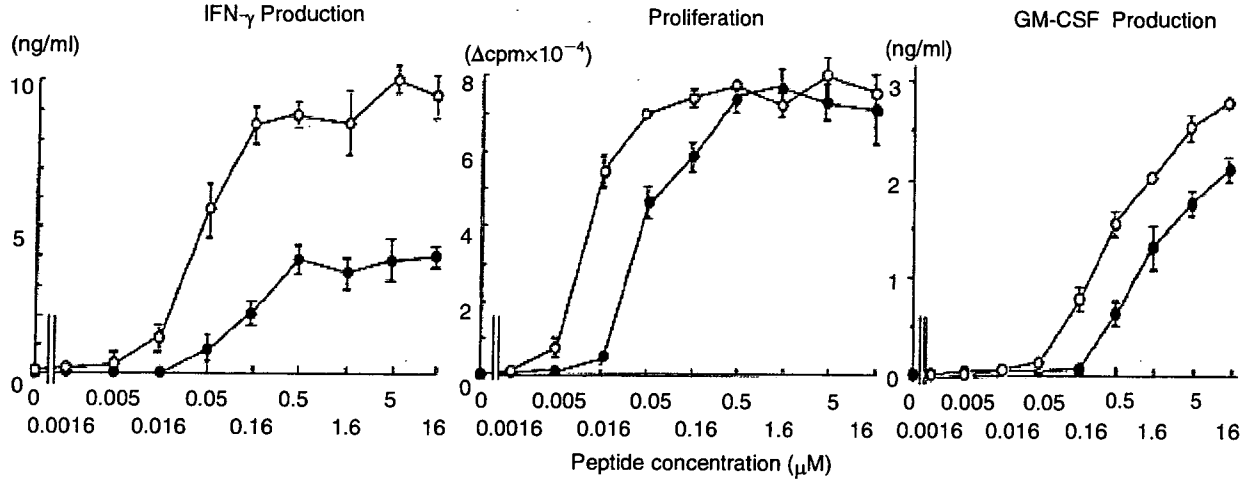

Fig. 1 IFN-γ production, GM-CSF production and proliferation of BC20.7 in recognition of either the wild-type peptide or L87V, at different concentrations. BC20.7 cells were cultured in triplicate with peptides and irradiated autologous PBMC, at the indicated concentrations. After 48-h incubation, supernatant fluids of triplicate cultures were collected. The remaining cells were pulsed with [^{3}H]-thymidine, harvested after 16h, and subjected to liquid scintillation counting. Closed circle, wild type peptide; open circle, L87V. Results are expressed as the geometric means ± standard error. IFN-γ production induced by L87V was significantly ($p<0.01$) higher than that induced by the wild-type peptide, at peptide concentrations ranging from 0.016 to 16 μM. On the other hand, plateau level of proliferation did not exhibit a significant difference, between 0.16 and 16 μM ($p>0.05$). GM-CSF production did not reach a plateau response even at 16 μM, without any statistical difference between L87V and the wild-type peptide, at 16 μM.

also observed when P5- and P8-substituted analogues were tested. Thus, S90E,S90G,S90M,D93Q,D93T and D93Y exhibited full agonism, in a clone-specific manner.

DISCUSSION

It is not very easy to identify TCR genes used by T cell clones, since they are usually cultured with irradiated autologous PBMC that includes polyclonal T cells. Random cloning of TCR cDNA derived from the cultured cells is minimally helpful in the identification, unless a large number of clones are examined. This problem was circumvented by the use of PCR-ELISA that was developed for TCRBV use,[9] and established in the present report for TCRVA usage. This technique allowed us to quantitate TCRV gene usage in the cDNA samples, and thus to identify the TCRV gene used by the T cell clones.

Three T-cell clones used in the present study recognize the same TCR ligand, as proven in our previous study. This is based on the fact that these clones recognize BCGa p84-100(^{84}EEYLILSARDVLAVVSK^{100}) in the context of DRB1*1405, and react to truncated peptides in a similar fashion.[11] Both BC20.7 and BC33.5 have 8 and 11 residues at N(D)N region of TCRVA and VB, respectively, whereas BC42.1 alone exhibits a different pattern, *i.e.*, 9 residues at N(D)N regions of TCRVA and VB. When peptide antigen is presented by class II MHC molecules, the N-terminal half of antigenic peptide is recognized mainly by CDR3 of TCRVA, whereas the C-terminal half is recoginized by CDR3 of TCRVB, which corresponds to N(D)N regions.[12] Interestingly, certain amino acid replacements on P2 induced increased IFN-γ production in BC20.7 and BC33.5 but not in BC42.1 cells, whereas those on P8 exhibited full agonism in BC 42.1 cells alone. It is thus likely that structural features of VACDR3 and VBCDR3 are responsible for specific responses induced by P2 and P8 analogues, respectively. Shuffling of N(D)N sequences between BC 42.1 and BC 20.7, or between BC 42.1 and BC 33.5 is underway to address this point.

Only L87T,L87S,L87A,and L87V induced IFN-γ enhancement. These arrangements are either smaller hydrophobic (A and V), or structurally similar neutral amino acids (T and S), indicating that close contact between P2 and TCRVA is taking place. Indeed, such a phenomenon is also seen in B-cell somatic hypermuation.[13] Thus, B-cell V region mutation in immunoglobulin heavy chain genes shows higher affinity than the germ-line sequence, usually associated with Gly, Ala, Val, Ser, Thr, or Cys, *i.e.*, small hydrophobic or small neutral residues. Apparently these mutations are not associated with static charges, but can affect either hydrogen bonding, van der Waar's force, or hydrophobic interactions.

In our previous studies using cedar pollen-derived peptides, T to V replacement on P2 also induced IFN-

Table 3 Increased IFN-γ production induced by peptide analogues

Replaced by	Relative IFN-γ response (BC20.7 / BC33.5 / BC42.1)								
	P1 =86Y	P2 =87L	P3 =88I	P4 =89L	P5 =90S	P6 =91A	P7 =92R	P8 =93D	P9 =94V
K	*/*/*	*/*/*	*/*/*	*/*/*	*/*/*	*/*/*	108/115/90	*/*/*	*/*/*
E	*/*/*	*/*/*	*/*/*	*/*/*	*/105/94	*/*/*	*/*/*	*/*/*	*/*/*
Q	*/*/*	88/79/90	*/*/*	92/79/81	*/*/*	*/*/*	*/*/*	*/*/87	*/*/*
N	*/*/*	105/97/95	*/*/*	88/92/97	*/*/*	*/*/*	*/*/*	*/*/*	*/*/*
T	*/*/*	177/210/86	110/92/81	*/*/*	77/97/108	*/*/*	*/*/*	*/*/95	85/96/91
S	*/*/*	155/187/90	95/95/99	*/*/*	100/100/100	81/87/97	*/*/*	*/*/*	93/75/99
G	*/*/*	110/98/79	90/100/92	*/*/*	*/*/115	77/69/93	*/*/*	*/*/*	94/99/100
A	96/100/98	189/202/94	105/94/83	107/93/83	88/104/110	100/100/100	*/*/*	*/*/*	80/81/92
V	91/91/85	271/259/92	91/84/86	105/96/86	99/100/101	90/76/85	*/*/*	*/*/*	100/100/100
L	93/88/102	100/100/100	100/90/101	100/100/100	*/*/*	*/*/*	*/*/*	*/*/*	*/*/*
Y	100/100/100	*/*/*	*/*/*	*/*/*	*/*/*	*/*/*	*/*/*	*/*/98	*/*/*
M	89/93/91	*/*/*	96/99/103	89/70/85	*/91/*	*/*/*	*/*/*	*/*/*	*/*/*
W	90/103/109	*/*/*	*/*/*	*/*/*	*/*/*	*/*/*	*/*/*	*/*/*	*/*/*

Positions 1 – 9 (P1 – P9) of BCGa p84-100 (EEYLILSARDVLAVVSK; with P1 underlined), was replaced by indicated amino acids. T cells were stimulated with peptide species at 16 μM. To obtain relative IFN-γ response values, plateau responses of IFN-γ (pg/ml) were first divided by plateau responses of proliferation (cpm). Then, the following calculation was performed; relative IFN-γ responses= 100x[IFN-γ/proliferation to analogues]/[IFN-γ/proliferation to the wild-type BCGa p84-100]. The denominator was 0.0533. *Peptide that did not induce fully agonistic proliferation.

γ enhancement, whereas proliferation remained the same. Therefore, although not generalized, mutual replacement on G, A, V, L, S, or T at P2, tends to induce IFN-γ-specific enhancement. Such observations also have been reported in another study with different peptide species.[14] In this sense, analogue-induced clonal anergy is often observed, especially when residue replacement is made on P7 or P8.[11] Moreover, truncation of the C-terminal moiety of antigenic peptides, in general, exhibit TCR antagonism.[15] In other words, if a rule that applies to altered polyclonal novel responses induced by peptide analogues is established, it will lead us to novel therapeutic interventions using peptide analogues. Our observations on P2 replacement which is associated with increased IFN-γ production are imperative to furthering our understanding.

ACKNOWLEDGEMENTS

This work was supported by the Ministry of Health, Labour and Welfare, Japan.

REFERENCES

1. Evavold BD, Allen PM. Separation of IL-4 production from Th cell proliferation by an altered T cell receptor ligand. *Science* 1991;**252**:1308.
2. Chen Y-Z, Matsushita S, Nishimura Y. Response of a human T cell clone to a large panel of altered peptide ligands carrying single residue substitutions in an antigenic peptide : characterization and frequencies of TCR agonism and TCR antagonism with or without partial activation. *J. Immunol.* 1996;**13**:3783-3790.
3. Sloan-Lancaster J, Evavold BD, Allen PM. Induction of T-cell anergy by altered T-cell-recepter ligand on live antigen-presenting cells. *Nature* 1993;**363**:156.
4. Matsushita S, Kohsaka H, Nishimura Y. Evidence for self- and non-self- peptide partial agonists that prolong clonal survival of mature T cells in vitro. *J. Immunol.* 1997;**158**: 5685-5691.
5. Ikagawa S, Matsushita S, Chen Y-Z, Ishikawa T, Nishimura Y. Single amino acid substitutions on a Japanese cedar pollen allergen (Cry j I)- derived peptide induced qualitative changes in human T cell responses and T cell receptor antagonism. *J. Allergy Clin. Immunol.* 1996;**97**:53-67.
6. Windhagen A, Scholz C, Höllsberg P, Fukaura H, Sette A, Hafler DA. Modulation of cytokine patterns of human autoreactive T cell clones by a single amino acid substitution of their peptide ligand. *Immunity* 1995;**2**:373.
7. Stern LJ, Brown JH, Jardetzky TS *et al.* Crystal structure of the human class II MHC protein HLA-DR1 complexed with an influenza virus peptide. *Nature* 1994;**368**:215-221.
8. Matsushita S, Yokomizo H, Kohsaka H, Nishimura Y. Diversity of a human $CD4^+$ T cell repertoire recognizing one TCR ligand. *Immunol. Lett.* 1996;**51**:191.
9. Kohsaka H, Taniguchi A, Chen PP, Ollier WER, Carson DA. The expressed T cell receptor V gene repertoire of rheumatoid arthritis monozygotic twins : rapid analysis by anchored polymerase chain reaction and enzyme-linked immunosorbent assay. *Eur. J. Immunol.* 1993;**23**: 1895-1901.
10. Nanki T, Kohsaka H, Mizushima N, Carson DA, Miyasaka N. Genetic control of human TCRBJ gene repertoires of peripheral T lymphocytes of normal and rheuma-

toid arthritis monozygotic twins. *J. Clin. Invest.* 1996;**98**: 1594-1601.

11. Matsushita S, Nishimura Y. Partial activation of human T cells by peptide analogs on live APC : induction of clonal anergy associated with protein tyrosine dephosphorylation. *Hum. Immunol.* 1997;**53**:73-80.

12. Hennecke J, Carfi A, Wiley DC. Structure of a covalently stabilized complex of a human αβ T-cell receptor, influenza HA peptide and MHC class II molecule, HLA-DR1. *EMBO J.* 2000;**19**:5611-5624.

13. Rogozin IB, Kolchanov NA. Somatic hypermutagenesis in immunoglobulin genes. II. Influence of neighbouring base sequences on mutagenesis. *Biochem. Biophys. Acta.* 1992;**1171**:11.

14. Yssel H, Johnson KE, Schneider PV. T cell activation-inducing epitope on the house dust mite allergen Der p 1. Proliferation and lymphokine production patterns by Der p 1-specific CD4+ T cell clones. *J. Immunol.* 1992;**148**: 738-745.

15. Matsushita S, Matsuoka T. Peptide length-dependent TCR antagonism on class II HLA-restricted responses of PBMC and T-cell clones. *Eur. J. Immunol.* 1999;**29**:431-436.

Inhibition of CX3CL1 (Fractalkine) Improves Experimental Autoimmune Myositis in SJL/J Mice[1]

Fumihito Suzuki,* Toshihiro Nanki,[2]* Toshio Imai,† Hirotoshi Kikuchi,‡ Shunsei Hirohata,‡ Hitoshi Kohsaka,* and Nobuyuki Miyasaka*

Idiopathic inflammatory myopathy is a chronic inflammatory muscle disease characterized by mononuclear cell infiltration in the skeletal muscle. The infiltrated inflammatory cells express various cytokines and cytotoxic molecules. Chemokines are thought to contribute to the inflammatory cell migration into the muscle. We induced experimental autoimmune myositis (EAM) in SJL/J mice by immunization with rabbit myosin and CFA. In the affected muscles of EAM mice, CX3CL1 (fractalkine) was expressed on the infiltrated mononuclear cells and endothelial cells, and its corresponding receptor, CX3CR1, was expressed on the infiltrated CD4 and CD8 T cells and macrophages. Treatment of EAM mice with anti-CX3CL1 mAb significantly reduced the histopathological myositis score, the number of necrotic muscle fibers, and infiltration of CD4 and CD8 T cells and macrophages. Furthermore, treatment with anti-CX3CL1 mAb down-regulated the mRNA expression of TNF-α, IFN-γ, and perforin in the muscles. Our results suggest that CX3CL1-CX3CR1 interaction plays an important role in inflammatory cell migration into the muscle tissue of EAM mice. The results also point to the potential therapeutic usefulness of CX3CL1 inhibition and/or blockade of CX3CL1-CX3CR1 interaction in idiopathic inflammatory myopathy. ***The Journal of Immunology*****, 2005, 175: 6987–6996.**

Idiopathic inflammatory myopathy (IIM),[3] including polymyositis and dermatomyositis, is characterized by chronic inflammation of the voluntary muscles associated with infiltration of inflammatory cells, including CD4 and CD8 T cells and macrophages, in the skeletal muscle (1–3). Infiltrated CD4 and CD8 T cells express cytotoxic molecules, such as perforin and granzyme granules, and the T cells and macrophages express inflammatory cytokines, such as TNF-α and IFN-γ (4–8). Therefore, the infiltrated inflammatory cells might play an important role in the pathogenesis of IIM. The inflammatory cell migration into the muscle is thought to involve the interaction of chemokines and chemokine receptors (9–14).

Chemokines are involved in leukocyte recruitment and activation at the site of inflammatory lesion (15). Approximately 50 chemokines have been identified to date, and they are classified into four subfamilies, C, CC, CXC, and CX3C chemokines, based on the conserved cystein motifs (16). Although the majority of chemokines are small secreted molecules, CX3CL1 (fractalkine) is expressed on the cell surface as a membrane-bound molecule (17, 18). The membrane-bound CX3CL1 is expressed on endothelial cells stimulated with TNF-α, IL-1, and IFN-γ (19–21), induces adhesion of the leukocytes, and supports leukocyte transmigration into tissue (22, 23). The soluble form of CX3CL1 is generated by proteolytic cleavage at a membrane-proximal region of the membrane-bound CX3CL1 by TNF-α-converting enzyme (a disintegrin and metalloproteinase domain 17) and a disintegrin and metalloproteinase domain 10 (24, 25), and is known to induce leukocyte migration (23). In contrast, CX3CR1, a unique receptor for CX3CL1, is expressed on peripheral blood CD4 and CD8 T cells that express cytotoxic molecules and type 1 cytokines (26, 27). CX3CR1 is also expressed on monocytes/macrophages, NK cells, and dendritic cells (28, 29).

Based on the infiltration of CTLs and macrophages into the affected muscles in patients with IIM, we speculated that the CX3CL1-CX3CR1 interaction might contribute to the inflammatory cell migration. In the present study we induced experimental autoimmune myositis (EAM) in SJL/J mice and examined CX3CL1 and CX3CR1 expression in the affected muscle of EAM mice. Furthermore, we studied the effect of CX3CL1 inhibition on EAM mice.

Materials and Methods

Induction of EAM

Male 5-wk-old SJL/J mice were purchased from Charles River Japan. Purified myosin from rabbit skeletal muscle (6.6 mg/ml; Sigma-Aldrich) was emulsified with an equal amount of CFA (Difco Laboratories) with 3.3 mg/ml *Mycobacterium butyricum* (Difco Laboratories). Mice were immunized intracutaneously with 100 μl of emulsion into four locations (total, 400 μl) on the back on days 0, 7, and 14. On day 21, the mice were killed, and the quadriceps femoris muscles were harvested. The muscle tissues were frozen immediately in chilled isopentane precooled in liquid nitrogen, and then 6-μm-thick cryostat sections were prepared at intervals of 200 μm. The sections were stained with H&E or used for immunohistochemistry. The experimental protocol was approved by the institutional animal care and use committee of Tokyo Medical and Dental University.

Immunohistochemistry

Immunohistological staining was performed as described previously (26, 30) with some modifications. Briefly, 6-μm-thick sections were air-dried and fixed in cold acetone at −20°C for 3 min. After air-drying at room

*Department of Medicine and Rheumatology, Tokyo Medical and Dental University Graduate School, Tokyo, Japan; †KAN Research Institute, Kyoto, Japan; and ‡Department of Internal Medicine, Teikyo University School of Medicine, Tokyo, Japan

Received for publication January 4, 2005. Accepted for publication September 1, 2005.

The costs of publication of this article were defrayed in part by the payment of page charges. This article must therefore be hereby marked *advertisement* in accordance with 18 U.S.C. Section 1734 solely to indicate this fact.

[1] This work was supported in part by a grant-in-aid from the Japan Intractable Diseases Research Foundation; the Fund for Intractable Diseases Research by Atsuko Ouchi from Tokyo Medical and Dental University; the Ministry of Health, Labor, and Welfare; and the Ministry of Education, Science, Sports, and Culture, Japan.

[2] Address correspondence and reprint requests to Dr. Toshihiro Nanki, Department of Medicine and Rheumatology, Tokyo Medical and Dental University Graduate School, 1-5-45, Yushima, Bunkyo-ku, Tokyo 113-8519, Japan. E-mail address: nanki.rheu@tmd.ac.jp

[3] Abbreviations used in this paper: IIM, idiopathic inflammatory myopathy; EAM, experimental autoimmune myositis; PTX, pertussis toxin.

0022-1767/05/$02.00

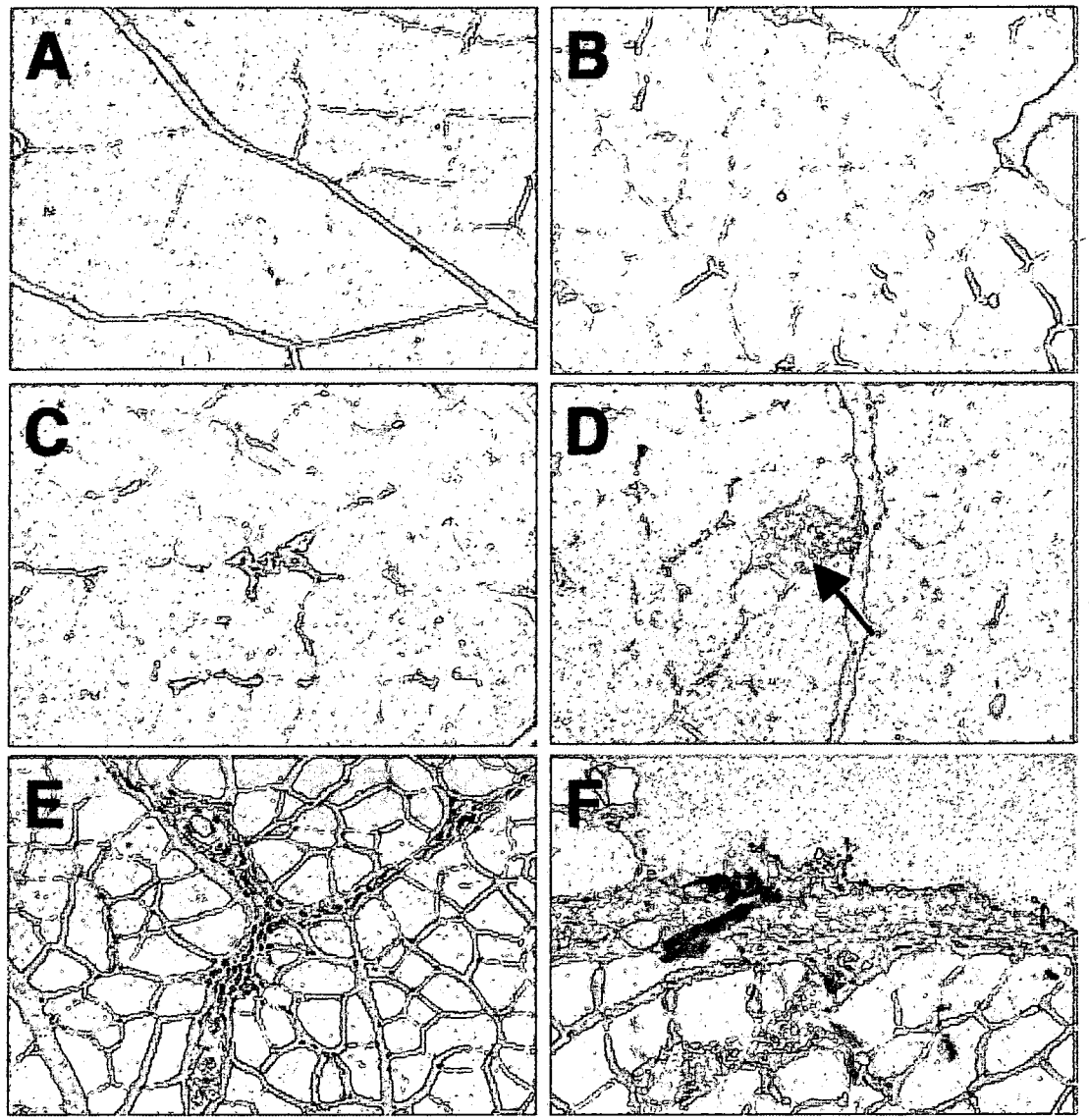

FIGURE 1. Histological changes found in the muscle of murine EAM. Quadriceps femoris muscle of normal mice and immunized mice on day 7 showed no inflammatory changes (*A* and *B*, respectively). On day 14, mild cellular infiltration in the muscle tissue was shown (*C*). Muscle tissues of EAM mice on day 21 showed cellular infiltration in the endomysium (*D*), perimysium (*E*), epimysium (*F*), and necrotic muscle fibers (arrow in *D*). H&E staining was used. Original magnification, ×200.

temperature, the slides were rehydrated in PBS for 2 min three times, and then the endogenous peroxidase activity was blocked by incubation in 1.0% H_2O_2 in PBS for 10 min, followed by rinsing for 2 min three times in PBS. Nonspecific binding was blocked with 10% normal rabbit serum in PBS for 30 min. For CD4, CD8, and F4/80 staining, the sections were incubated with 5 μg/ml rat anti-mouse CD4 mAb (GK1.5; Cymbus Biotechnology), 2 μg/ml rat anti-mouse CD8a mAb (53-6.7; BD Pharmingen), 5 μg/ml rat anti-mouse F4/80 mAb (C1:A3-1; Serotec), or normal rat IgG in Ab diluent (BD Pharmingen) overnight at 4°C. The samples were then washed three times in PBS for 5 min each time and incubated with biotin-conjugated rabbit anti-rat IgG (DakoCytomation) for 30 min at room temperature with 5% normal mouse serum. To analyze a time course of cell infiltration, numbers of $CD4^+$, $CD8^+$, and $F4/80^+$ cells in six randomly selected fields at ×200 were counted from three EAM mice on days 0, 7, 14, and 21.

For mouse vascular endothelial cell staining, we used a tyramide signal amplification kit (NEL700A; PerkinElmer). After blocking with 10% normal rabbit serum, the sections were incubated with 5 μg/ml rat anti-mouse vascular endothelial cadherin Ab (11D4.1; BD Pharmingen) or normal rat IgG overnight at 4°C. The samples were then washed three times in PBS for 5 min each time and incubated with biotin-conjugated rabbit anti-rat IgG for 30 min at room temperature with 5% normal mouse serum. After washing three times in PBS for 5 min each time, the sections were incubated with streptavidin-HRP for 30 min at room temperature and washed in PBS three times for 5 min each time. The samples were incubated with biotinyl tyramide amplification reagent at room temperature for 5 min, then washed three times in PBS for 5 min each time, and incubated again with streptavidin-HRP for 30 min. After washing three times in PBS for 5 min each time, diaminobenzidine tablets (Sigma-Aldrich) were used for visualization. The sections were counterstained in hematoxylin for 30 s and washed in tap water for 5 min.

For mouse CX3CL1 staining, the endogenous peroxidase activity was blocked by incubation in 1.0% H_2O_2 in methanol, and then the sections were incubated overnight at 4°C with goat anti-mouse CX3CL1 Ab (sc-7227; Santa Cruz Biotechnology) or normal goat IgG in Ab diluent at 5 μg/ml. The samples were then washed three times in PBS for 5 min each time and incubated with biotin-conjugated rabbit anti-goat IgG (DakoCytomation) for 30 min at room temperature with 5% normal mouse serum. After washing three times in PBS for 5 min each time, the sections were incubated with peroxidase-conjugated streptavidin (DakoCytomation) for 30 min at room temperature and washed three times for 5 min each time. For enhancing the expression of CX3CL1 on endothelial cells, a tyramide signal amplification kit was

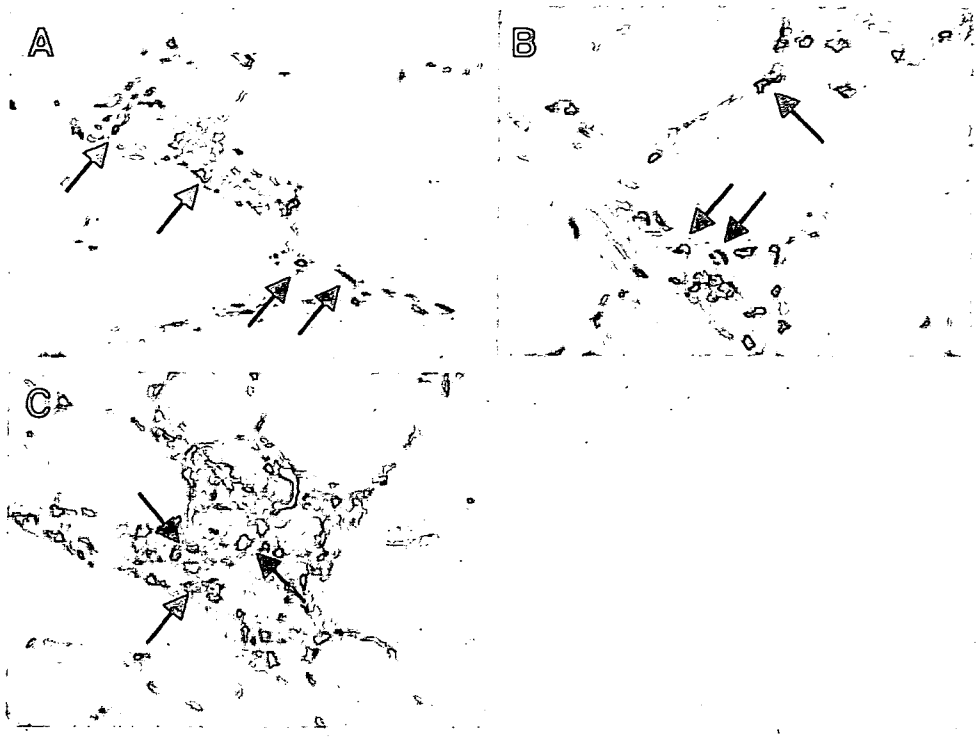

FIGURE 2. Infiltration of CD4 and CD8 T cells and macrophages in the muscles of EAM mice. Frozen sections of the quadriceps femoris muscle of EAM mice on day 21 were examined by immunohistochemistry using mAb against CD4 (*A*), CD8 (*B*), and F4/80 (*C*). The arrows indicate $CD4^+$, $CD8^+$, and $F4/80^+$ cells. Original magnification, ×200.

used as described above. Diaminobenzidine tablets were used for visualization. The sections were counterstained in hematoxylin for 30 s and washed in tap water for 5 min.

For CD4, CD8 or F4/80, and CX3CR1 double staining, the sections were incubated overnight at 4°C with 5 μg/ml rat anti-mouse CD4 mAb (GK1.5), 5 μg/ml rat anti-mouse CD8 mAb (53-6.7), 5 μg/ml rat anti-mouse F4/80 mAb (C1:A3-1), or normal rat IgG in Ab diluent. Subsequently, the samples were washed three times for 5 min each time in PBS and incubated with Alexa Fluor 488-conjugated goat anti-rat IgG (Molecular Probes) at 5 μg/ml for 1 h at room temperature. For CX3CR1 staining, the sections were washed three times in PBS for 5 min each time and then incubated with rabbit anti-mouse CX3CR1 Ab (30) or normal rabbit IgG at 5 μg/ml in Ab diluent for 2 h at room temperature. Next, the samples were washed three times for 5 min each time in PBS and incubated with Alexa Fluor 568-conjugated goat anti-rabbit IgG (Molecular Probes) at 5 μg/ml for 1 h at room temperature. The slides were examined using fluorescent microscopy (BZ-Analyzer; Keyence).

Treatment with anti-mouse CX3CL1 mAb

A mAb against murine CX3CL1 was generated from Armenian hamsters immunized with recombinant murine CX3CL1 by a standard method. One mAb, 5H8-4, was selected for additional studies. The specificity was examined by ELISA using a panel of murine CXC (MIP-2, keratinocyte-derived chemokine, and CXCL9, 10, 12, and 13), CC (CCL1–7, 9–12, 17, 19–22, 25, 27, and 28), C (XCL1), and CX3C (CX3CL1) chemokines. The mAb reacted specifically with murine CX3CL1. Five hundred micrograms of hamster anti-mouse CX3CL1 mAb (5H8-4) or control Ab (hamster IgG; ICN Pharmaceuticals) was injected into the mouse peritoneal cavity three times per week from day 0 for 3 wk. The injection of anti-CX3CL1 mAb did not affect the number of PBMC (data not shown).

The severity of inflammatory changes was classified using five grades according to the classification of Kojima et al. (31) with some modification: score 0, no inflammation; score 1, mild endomysial inflammatory changes; score 2, severe endomysial inflammatory changes; score 3, perimysial inflammatory changes in addition to score 2; and score 4, diffuse extensive lesion. If multiple lesions were found in one muscle specimen, 0.5 point was added to the indicated score. To evaluate the severity of inflammation using a different aspect, we counted the number of necrotic muscle fibers, and $CD4^+$, $CD8^+$, and $F4/80^+$ cells in continuous three sections. Each section examined six random fields at ×400. The evaluation of histopathological inflammatory changes was performed in a blind fashion for the experimental group identity.

Real-time RT-PCR

Total RNA was prepared from a 100 mg muscle block using RNA extraction solution, Isogen (Nippon Gene), and treated with DNase I (Invitrogen Life Technologies). The first-strand cDNA was synthesized using oligo$(dT)_{12-18}$ primers (Pharmacia Biotech) and SuperScript II reverse transcriptase (Invitrogen Life Technologies).

The relative quantitative real-time PCR was performed using SYBR Green I on ABI PRISM 7000 (Applied Biosystems) according to the instructions provided by the manufacturer. The cDNA was amplified with primers for TNF-α (5′, GTA CCT TGT CTA CTC CA GGT TCT CT; 3′, GTG TGG GTG AGG AGC ACG TA), IFN-γ (5′, CCT GCG GCC TAG CTC TGA; 3′, CCA TGA GGA AGA GCT GCA AAG), perforin (5′, CCA CGG CAG GGT GAA ATT C; 3′, GGC AGG TCC CTC CAG TGA), and GAPDH (5′, ATG CAT CCT GCA CCA CCA A; 3′, GTC ATG AGC CCT TCC ACA ATG). These primers were designed using the ABI Primer Express Software program (Applied Biosystems). The reaction buffer contained the following components: 25 μl of SYBR Green PCR Master Mix (Applied Biosystems), 300 nM forward and reverse primers, 50 ng cDNA template, and RNA-free distilled water up to 50 μl of total volume. The PCR was conducted using the following parameters: 50°C for 2 min, 95°C for 10 min, and 40 cycles of denaturation at 95°C for 15 s and annealing/extension at 60°C for 1 min. GAPDH mRNA was used as an internal control to standardize the amount of sample mRNA. A validation experiment demonstrated approximately equal efficiencies of the target and reference. Thus, the relative expression of real-time PCR products was determined using the ΔΔCt method that compares the mRNA expression levels of the target gene and the housekeeping gene (32, 33). One of the control samples was chosen as a calibrator sample.

Statistical analysis

Differences in the score of tissue inflammation, number of necrotic muscle fibers, number of migrated cells, and relative expression levels of TNF-α, IFN-γ, and perforin between control Ab- and anti-mouse CX3CL1 mAb-treated EAM mice, and the relative expression levels of TNF-α, IFN-γ, and perforin between normal and EAM mice were examined for statistical significance using Mann-Whitney's *U* test. All data were expressed as the

mean ± SEM. The difference between two groups of mice was considered significant at $p < 0.05$.

Results

Development of EAM

SJL/J mice were immunized with purified rabbit myosin fraction and CFA on days 0, 7, and 14. On days 0, 7, 14, and 21, the quadriceps femoris muscles of these mice were histologically examined with H&E staining. All muscle specimens of normal SJL/J mice and immunized mice on day 7 showed normal appearance with no inflammatory changes (Fig. 1, *A* and *B*, respectively), whereas those of mice immunized with rabbit myosin fraction showed mild mononuclear cell infiltration at day 14 (Fig. 1*C*). On day 21, a significant number of mononuclear cells were infiltrated among the muscle fibers (endomysium; Fig. 1*D*), at perivascular areas (perimysium; Fig. 1*E*), and epimysium (Fig. 1*F*). Scattered lesions with aggregates of infiltrated mononuclear cells were formed, in which atrophic or necrotic muscle fibers were noted (arrow in Fig. 1*D*). Injection of PBS and CFA into SJL/J mice did not show infiltration of inflammatory cells in the quadriceps femoris muscles (data not shown).

To determine the subsets of infiltrating mononuclear cells in the quadriceps femoris muscles of EAM mice, we performed immunohistochemical analysis using mAbs against CD4, CD8, and F4/80. $CD4^+$ T cells were mainly located in the perimysium and some were found in the endomysium (Fig. 2*A*). $CD8^+$ T cells were predominantly detected in the endomysium and surrounded nonnecrotic muscle fibers (Fig. 2*B*). $F4/80^+$ macrophages were located in the endomysium as well and were especially present around the necrotic muscle fibers (Fig. 2*C*). Because these histological findings of inflammatory cell infiltration patterns resembled those of affected muscle lesions in IIM patients (34–36), we decided to use the EAM mice as an experimental model of IIM.

To evaluate a time course of cellular infiltration into the muscles, we counted the numbers of infiltrated $CD4^+$, $CD8^+$, and $F4/80^+$ cells on days 0, 7, 14, and 21 by immunohistochemical method. The majority of the infiltrating cells on day 14 were $F4/80^+$ macrophage (Fig. 3). In contrast, the number of $CD4^+$ and $CD8^+$ T cells was not increased until day 14, and they had significantly migrated into the muscles on day 21. These results were similar to previously reported data (37).

CX3CL1 and CX3CR1 expression in the muscle of EAM mice

We examined the expression of CX3CL1 in the muscle of normal SJL/J mice and EAM mice by immunohistochemistry. In the quadriceps femoris muscles of normal mice, no CX3CL1 expression was detected (Fig. 4, *A* and *G*). In contrast, CX3CL1 was expressed on infiltrated mononuclear cells predominantly in the endomysium and vascular endothelial cells of EAM mice on day 14 (Fig. 4, *B* and *H*, respectively) and day 21 (Fig. 4, *C* and *I*, respectively).

We next examined the expression of CX3CR1 on the infiltrated mononuclear cells in the quadriceps femoris muscle of EAM mice by double immunohistochemical staining. Some $CD4^+$ T cells expressed CX3CR1 (Fig. 5, *A–C*). The majority of $CD8^+$ T cells and most of the $F4/80^+$ macrophages expressed CX3CR1 (Fig. 5, *D–F* and *G–I*, respectively).

Effect of anti-mouse CX3CL1 mAb on EAM mice

To analyze the effect of anti-CX3CL1 mAb administration on EAM mice, we evaluated the histological changes in quadriceps femoris muscle using H&E staining. The incidence of inflammatory cell infiltration in control Ab-treated mice was 100% ($n = 10$). Treatment with anti-CX3CL1 mAb did not change the incidence of cellular infiltration (100%; $n = 10$). EAM mice treated with control Ab showed mononuclear cell infiltration with atrophy and necrosis of muscle fibers (Fig. 6*A*). In comparison, anti-CX3CL1 mAb-treated EAM mice showed milder histological changes (Fig. 6*B*). Analysis of histological scores of inflammatory changes in the quadriceps femoris muscles indicated that treatment with anti-CX3CL1 mAb significantly reduced inflammatory cell infiltration in the muscles of EAM mice compared with treatment with control Ab (Fig. 6*C*). Moreover, anti-CX3CL1 mAb treatment reduced the number of necrotic muscle fibers in muscles (Fig. 6*D*). A similar result was obtained in another independent set of experiments.

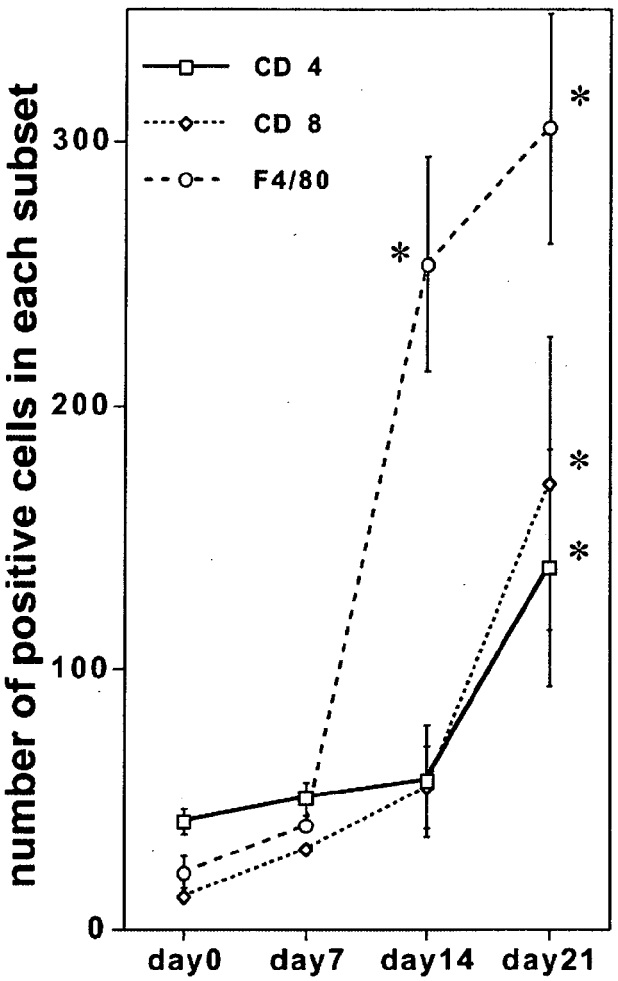

FIGURE 3. Time course of inflammatory cell infiltration into the muscle tissue of EAM mice. The numbers of infiltrating $CD4^+$, $CD8^+$, and $F4/80^+$ cells into the quadriceps femoris muscles were counted by immunohistochemistry. Data represent the mean ± SEM. *, $p < 0.05$.

We next examined the effect of anti-CX3CL1 mAb treatment on the numbers of each subset of infiltrating cells. The numbers of $CD4^+$, $CD8^+$, and $F4/80^+$ cells in quadriceps femoris muscles were counted and compared between mice treated with control Ab and those with anti-CX3CL1 mAb. Anti-CX3CL1 mAb treatment significantly reduced the number of infiltrated $CD4^+$ T cells by ~30% (Fig. 7*A*), $CD8^+$ T cells by ~50%, and $F4/80^+$ macrophages by up to 50% (Fig. 7, *B* and *C*).

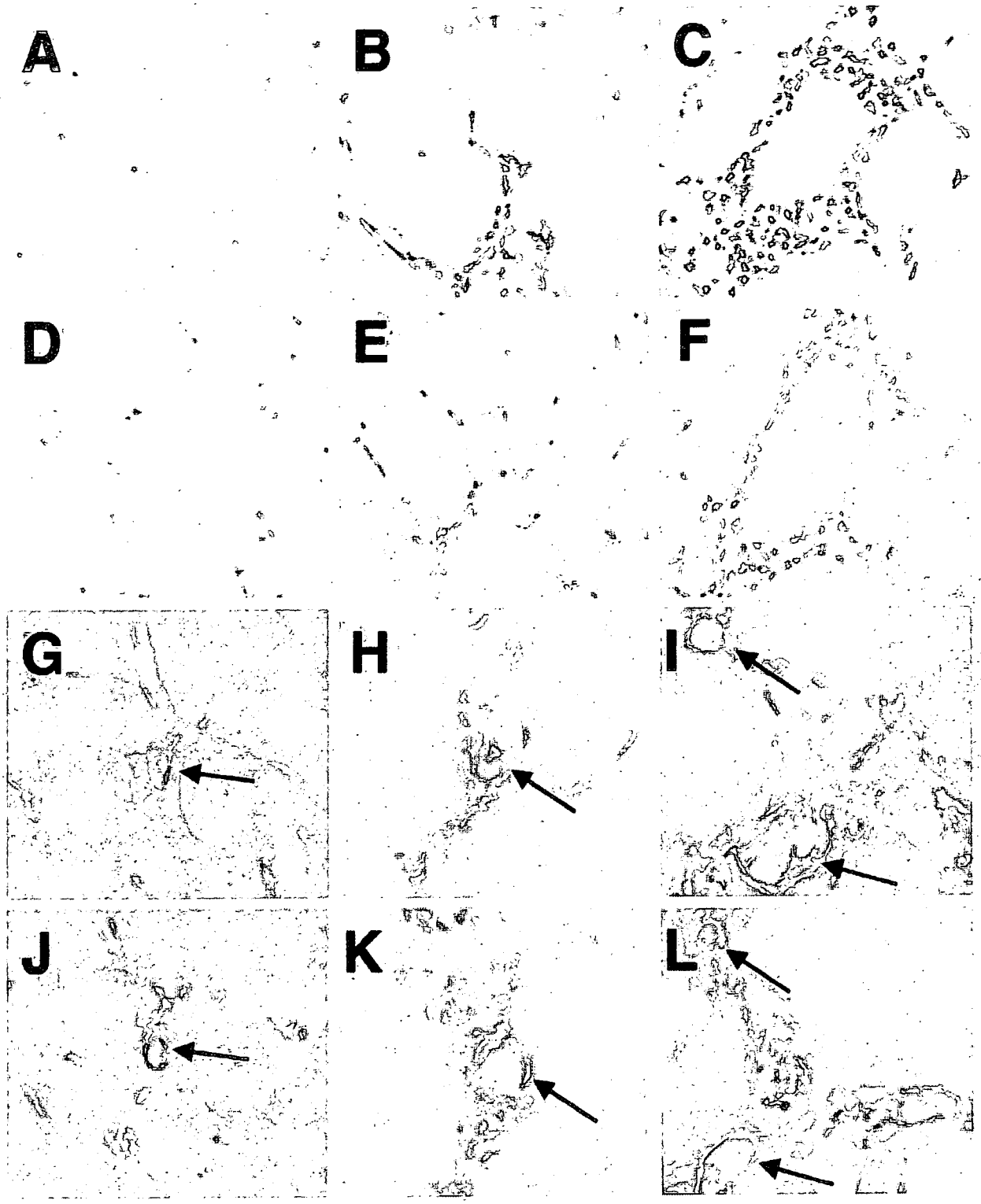

FIGURE 4. CX3CL1 expression in the muscles of EAM mice. Expression of CX3CL1 was examined by immunohistochemistry in normal mice (*A* and *G*) and EAM mice on day 14 (*B* and *H*) and day 21 (*C* and *I*). Vascular endothelial cadherin expression in the normal mice (*J*) and EAM mice on day 14 (*K*) and 21 (*L*) was also examined using serial sections with *G*, *H*, and *I*, respectively. Stainings with isotype control Ab for CX3CL1 are shown (*D*, normal mice; *E*, EAM on day 14; *F*, EAM on day 21). Arrows indicate vascular endothelial cadherin-positive endothelial cells (*J–L*), and corresponding endothelial cells (*G–I*). Original magnification, ×400.

We finally examined the effects of anti-CX3CL1 mAb treatment on the expression of cytokines and cytotoxic molecule in the quadriceps femoris muscle of EAM mice by quantitative RT-PCR. Although the relative quantities of TNF-α, IFN-γ, and perforin mRNA were very low in normal SJL/J mice, they were significantly up-regulated in EAM mice that received control Ab treatment ($p < 0.05$). Furthermore, treatment with anti-CX3CL1 mAb strikingly reduced mRNA expression (Fig. 8).

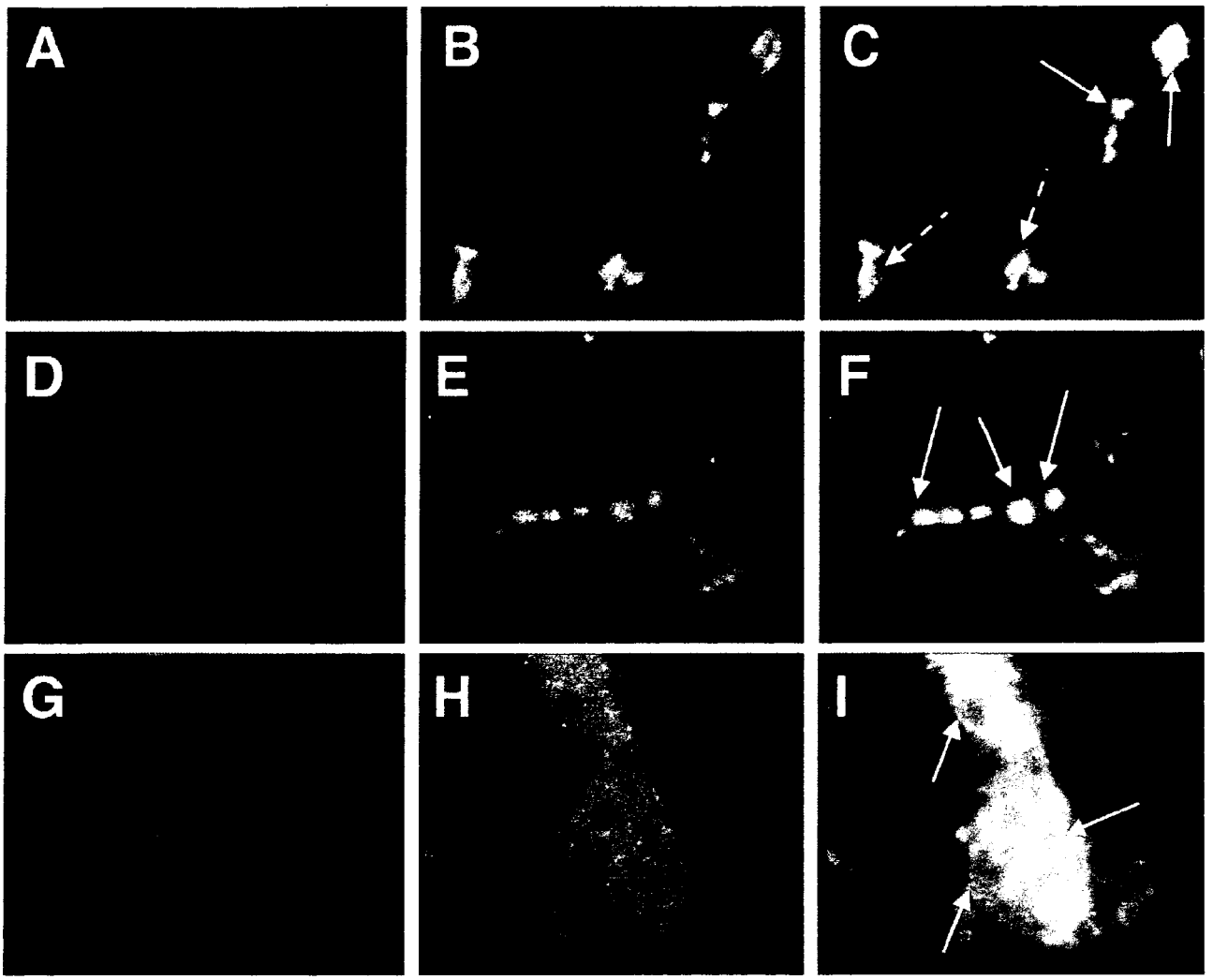

FIGURE 5. CX3CR1 expression on $CD4^+$, $CD8^+$, or $F4/80^+$ cells in the EAM muscle. Muscle tissues from EAM mice were double stained with CD4, CD8, or F4/80, and CX3CR1, and analyzed with fluorescent microscopy (*A*, CX3CR1; *B*, CD4; *C*, merged *A* and *B*; *D*, CX3CR1; *E*, CD8; *F*, merged *D* and *E*; *G*, CX3CR1; *H*, F4/80; *I*, merged *G* and *H*). Solid arrows indicate double-positive cells. Dotted arrows indicate CX3CR1-negative CD4 T cells. Original magnification, ×200.

Considered together, the above results indicate that treatment with anti-CX3CL1 mAb reduced infiltration of CD4 and CD8 T cells and macrophages and reduced the expression of various inflammatory cytokines and cytotoxic molecule in muscles.

Discussion

The major findings of the present study were the following. 1) CX3CL1 was expressed on infiltrated mononuclear cells and vascular endothelial cells, and its corresponding receptor, CX3CR1, was expressed on infiltrated inflammatory cells in the muscles of EAM. 2) Treatment with anti-CX3CL1 mAb ameliorated histological inflammatory changes in EAM mice, reduced the numbers of infiltrated CD4 and CD8 T cells and macrophages, and reduced the expression of TNF-α, IFN-γ, and perforin in the muscles. These results suggest that CX3CL1-CX3CR1 interaction seems to play an important role in inflammatory cell migration into the muscles of EAM mice.

Development of EAM in SJL/J mice by immunization with rabbit purified skeletal myosin fraction and CFA was previously reported (37–40). We modified the method by increasing the amount of immunized myosin and CFA and the addition of *Mycobacterium butyricum*. This modification shortened the period required for the development of myositis from 5 wk, which was thought to be appropriate for the induction (38), to 3 wk. Moreover, although pertussis toxin (PTX) injection into the peritoneal cavity increased the severity of inflammatory changes in the muscle (31), and thus, PTX was administered in the previous models (31, 36, 38), our modified method induces significant myositis without PTX injection. The EAM mice showed inflammatory cell infiltration in the endomysium, perimysium, and epimysium with muscle fiber necrosis. Immunohistochemical analysis showed that the invading cells surrounding nonnecrotic muscle fibers in the endomysium were mainly CD8 T cells, whereas macrophages were predominantly detected in necrotic fibers, and CD4 T cells were located in perimysium. Moreover, quantitative RT-PCR showed up-regulation of expression of TNF-α, IFN-γ, and perforin mRNA in the muscle of EAM mice. These findings in EAM mice are similar to those reported in IIM patients (4–8, 34–36).

Inflammatory cell migration into the affected muscle of IIM is thought to involve chemokine-chemokine receptor interaction

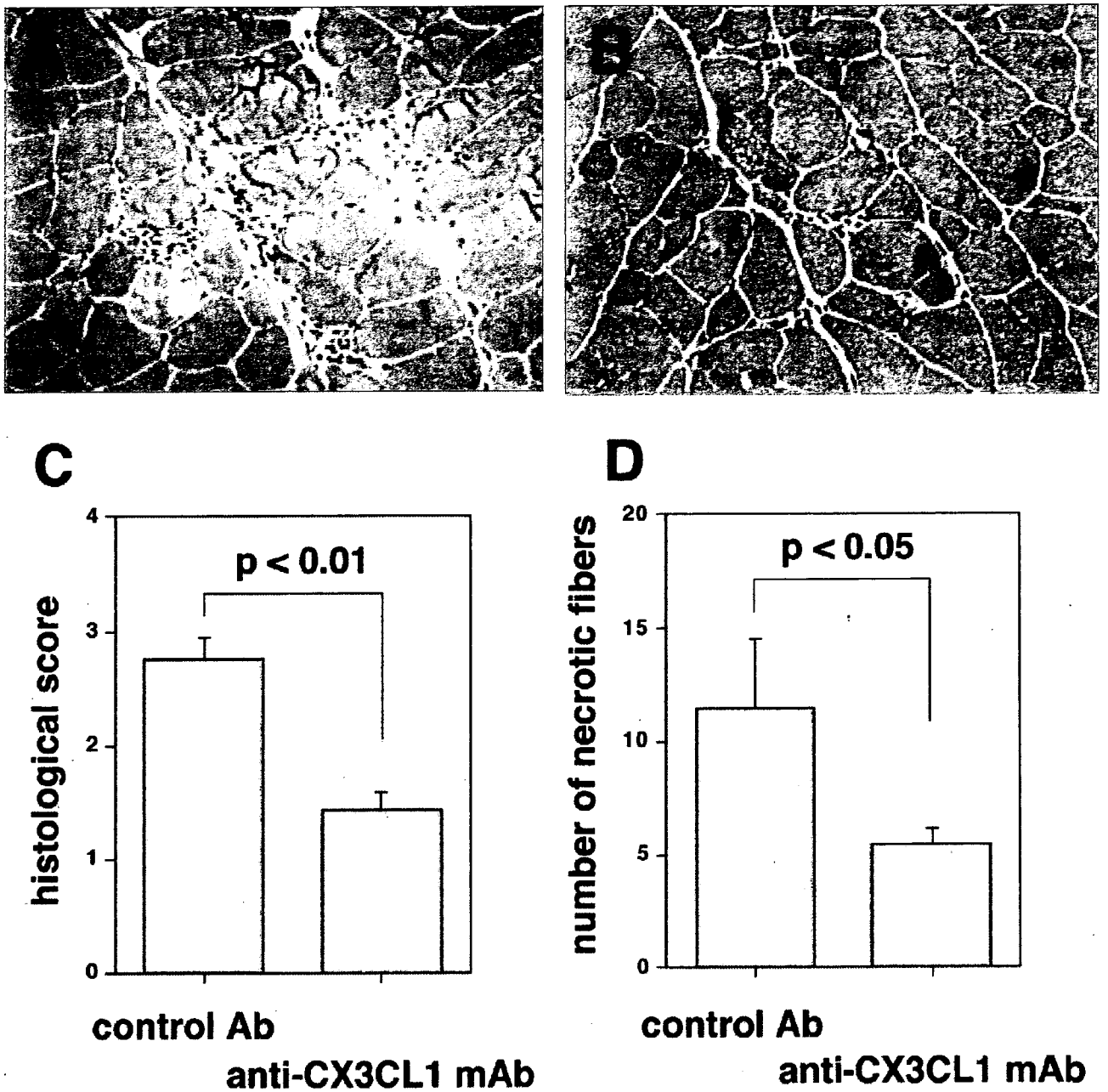

FIGURE 6. Inhibition of inflammatory changes in the muscle by treatment with anti-CX3CL1 mAb. Five hundred micrograms of hamster anti-mouse CX3CL1 mAb or control Ab was injected into the peritoneal cavity three times per week from day 0 for 3 wk. On day 21, the quadriceps femoris muscles of EAM mice were examined with H&E staining, histological scores were evaluated, and the numbers of necrotic fibers were counted. Mice treated with control Ab showed inflammatory cell accumulation (*A*). Mice treated with anti-CX3CL1 mAb showed milder inflammatory changes (*B*). Representative photomicrographs of histology from 10 animals in each group are shown. Histological scores of inflammatory changes in quadriceps femoris muscles were evaluated (*C*). The numbers of necrotic fibers were counted in the muscle tissues (*D*). Data represent the mean ± SEM.

(9–14). In the present study we focused on the role of CX3CL1-CX3CR1 interaction in the inflammatory cell migration. We showed the expression of CX3CR1 on some CD4 T cells and most CD8 T cells in EAM mice. It has been reported that CTLs including both $CD4^+$ and $CD8^+$ T cells invade the muscle fibers in IIM patients (3). These cells possess cytotoxic molecules, such as perforin and granzyme B, which are released into muscle cells (4, 5). Furthermore, type 1 cytokines, such as TNF-α and IFN-γ, were expressed in the inflammatory lesions of IIM patients (6–8). These findings suggest that the cytotoxic molecules and type 1 cytokines play important roles in the inflammatory lesions in IIM patients. In contrast, we reported previously that peripheral blood $CX3CR1^+$ T cells express cytotoxic molecules and type 1 cytokines (26, 27). Therefore, the interaction of CX3CL1 and CX3CR1 could induce the migration of T cells, which express cytotoxic molecules and type 1 cytokines, into the affected muscles.

The infiltrated macrophages into the affected muscle also express inflammatory cytokines (9, 41). They express TNF-α and IL-1β, which could stimulate T cells, macrophages, and

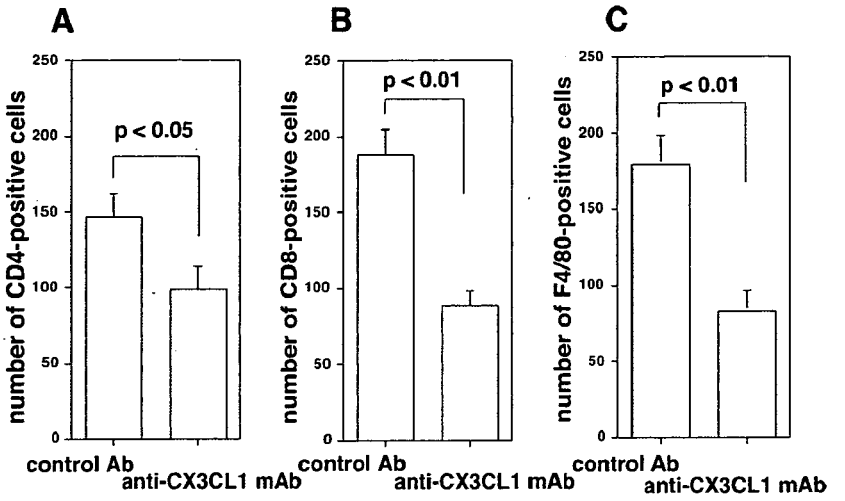

FIGURE 7. Decreased numbers of infiltrating cells of each subset by anti-CX3CL1 mAb treatment. Numbers of infiltrating $CD4^+$, $CD8^+$, and $F4/80^+$ cells were counted in the quadriceps femoris muscles from the experiment shown in Fig. 6. Data represent the mean ± SEM.

endothelial cells to produce various inflammatory cytokines, chemokines, and adhesion molecules. Moreover, these cytokines might have myocytotoxic effects (42–44). Our results showed that the majority of the $F4/80^+$ macrophages expressed CX3CR1 in the muscle of EAM mice. Thus, the CX3CL1-CX3CR1 interaction might also play an important role in macrophage migration into the affected muscle in addition to T cell migration.

CX3CL1 was expressed on infiltrated mononuclear cells in the affected muscles of EAM mice. Because CX3CL1 expression was located in the endomysium, infiltrated macrophages and/or CD8 T cells may express CX3CL1 in the muscles. Furthermore, we showed that CX3CL1 was also expressed on vascular endothelial cells in the EAM muscle tissue on days 14 and 21, but not in normal mice. It was reported that CX3CL1 was expressed on endothelial cells activated with TNF-α and IFN-γ in vitro (19–21). Expressed CX3CL1 on endothelial cells might recruit $CX3CR1^+$ cells, including macrophages and T cells, into muscle. These cells, in turn, express TNF-α and IFN-γ, which induce additional CX3CL1 expression on endothelial cells and also on recruited inflammatory cells. The enhanced expression of CX3CL1 may induce additional inflammatory cell migration. Consequently, these amplification cascades could contribute to the expansion of pathological changes in EAM mice. In fact, inhibition of CX3CL1 reduced the numbers of migrated CD4 and CD8 T cells and macrophages in the affected muscles of EAM mice and also reduced the expression of TNF-α, IFN-γ, and perforin. These results suggest that CX3CL1 blockade reduces the migration of inflammatory cells, which express cytotoxic molecules and cytokines, into the muscles. Thus, inhibition of CX3CL1-CX3CR1 interaction might be a potentially suitable therapeutic strategy for treatment of IIM.

Our data showed that mRNA expression of TNF-α, IFN-γ, and perforin was almost totally inhibited by anti-CX3CL1 mAb treatment, although the numbers of infiltrated monocytes were decreased by up to 50%. Recently it was reported that stimulation with CX3CL1 enhanced production of proinflammatory cytokines such as IFN-γ as well as the release of cytolytic granules by T cells (45). Thus, blockade of CX3CL1 might inhibit not only cellular migration, but also cytokine and cytotoxic molecule expression, by stimulation with CX3CL1 in the EAM muscle. Alternatively, because $CX3CR1^+$ T cells express type 1 cytokine and cytotoxic molecules (23, 26, 27), and $CX3CR1^{high}$ positive monocytes greatly produce inflammatory cytokines compared with $CX3CR1^{low}$ positive monocytes (46–48), treatment with anti-CX3CL1 mAb may selectively inhibit the migration of such specific T cells and macrophages. Therefore, anti-CX3CL1 mAb might be able to inhibit the expression of cytokine and cytotoxic molecules effectively in muscles, but additional study is required.

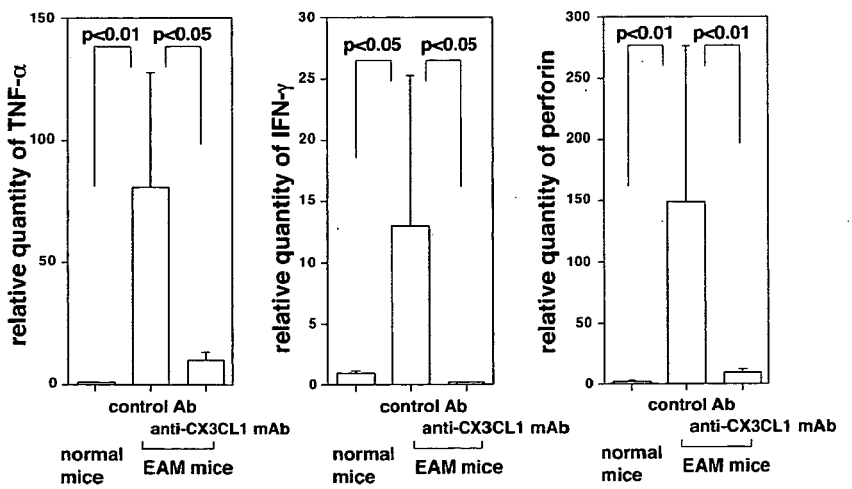

FIGURE 8. Reduction of TNF-α, IFN-γ, and perforin expression by anti-CX3CL1 mAb treatment. Expression of TNF-α, IFN-γ, and perforin mRNA in quadriceps femoris muscles from normal mice (n = 10) and from the experiment shown in Fig. 6 were measured using real-time RT-PCR. Data represent the mean ± SEM.

We recently reported that inhibition of CX3CL1 ameliorated collagen-induced arthritis in mice, probably by suppression of inflammatory cell migration into the synovium (30). Others reported that anti-CX3CR1 Ab treatment blocked inflammatory cell infiltration in the glomeruli, prevented crescent formation, and improved renal function in the Wistar-Kyoto crescentic glomerulonephritis model (49). Furthermore, the gene deletion of CX3CR1 resulted in an ~50% decrease in the formation of atherosclerotic lesions and the number of infiltrated macrophages in the lesion in experimental atherosclerosis mice (50, 51). These results together with our findings suggest that blockade of CX3CL1-CX3CR1 interaction might be therapeutically useful for several diseases associated with inflammatory cell infiltration. In this study we propose that such treatment is also suitable for IIM. To our knowledge, this is the first report demonstrating that a chemokine inhibitor could reduce the severity of myositis.

In conclusion, we demonstrated in the present study that inhibition of CX3CL1 significantly improved histopathological changes in the muscles of EAM mice, suggesting that blockade of CX3CL1 might be therapeutically beneficial for IIM.

Acknowledgments

We thank Dr. Hiroshi Nemoto (Toho University School of Medicine) for providing critical suggestions for the development of EAM mice. We also thank Miyuki Nishimura, Keiko Mizuno, and Yoko Inoue for their excellent technical support.

Disclosures

The authors have no financial conflict of interest.

References

1. Arahata, K., and A. G. Engel. 1984. Monoclonal antibody analysis of mononuclear cells in myopathies. I. Quantitation of subsets according to diagnosis and sites of accumulation and demonstration and counts of muscle fibers invaded by T cells. *Ann. Neurol.* 16: 193–208.
2. Engel, A. G., and K. Arahata. 1984. Monoclonal antibody analysis of mononuclear cells in myopathies. II. Phenotypes of autoinvasive cells in polymyositis and inclusion body myositis. *Ann. Neurol.* 16: 209–215.
3. Dalakas, M. C. 1991. Polymyositis, dermatomyositis and inclusion-body myositis. *N. Engl. J. Med.* 325: 1487–1498.
4. Cherin, P., S. Herson, M. C. Crevon, J. J. Hauw, P. Cervera, P. Galanaud, and D. Emilie. 1996. Mechanisms of lysis by activated cytotoxic cells expressing perforin and granzyme-B genes and the protein TIA-1 in muscle biopsies of myositis. *J. Rheumatol.* 23: 1135–1142.
5. Goebels, N., D. Michaelis, M. Engelhardt, S. Huber, A. Bender, D. Pongratz, M. A. Johnson, H. Wekerle, J. Tschopp, D. Jenne, et al. 1996. Differential expression of perforin in muscle-infiltrating T cells in polymyositis and dermatomyositis. *J. Clin. Invest.* 97: 2905–2910.
6. Tews, D. S., and H. H. Goebel. 1996. Cytokine expression profile in idiopathic inflammatory myopathies. *J. Neuropathol. Exp. Neurol.* 55: 342–347.
7. Lepidi, H., V. Frances, D. Figarella-Branger, C. Bartoli, A. Machado-Baeta, and J. F. Pellissier. 1998. Local expression of cytokines in idiopathic inflammatory myopathies. *Neuropathol. Appl. Neurobiol.* 24: 73–79.
8. Sugiura, T., Y. Kawaguchi, M. Harigai, K. Takagi, S. Ohta, C. Fukasawa, M. Hara, and N. Kamatani. 2000. Increased CD40 expression on muscle cells of polymyositis and dermatomyositis: role of CD40-CD40 ligand interaction in IL-6, IL-8, IL-15, and monocyte chemoattractant protein-1 production. *J. Immunol.* 164: 6593–6600.
9. Lundberg, I. E. 2000. The role of cytokines, chemokines, and adhesion molecules in the pathogenesis of idiopathic inflammatory myopathies. *Curr. Rheumatol. Rep.* 2: 216–224.
10. De Bleecker, J. L., B. De Paepe, I. E. Vanwalleghem, and J. M. Schroder. 2002. Differential expression of chemokines in inflammatory myopathies. *Neurology* 58: 1779–1785.
11. Liprandi, A., C. Bartoli, D. Figarella-Branger, J. F. Pellissier, and H. Lepidi. 1999. Local expression of monocyte chemoattractant protein-1 (MCP-1) in idiopathic inflammatory myopathies. *Acta Neuropathol.* 97: 642–648.
12. Confalonieri, P., P. Bernasconi, P. Megna, S. Galbiati, F. Cornelio, R. Mantegazza. 2000. Increased expression of β-chemokines in muscle of patients with inflammatory myopathies. *J. Neuropathol. Exp. Neurol.* 59: 164–169.
13. Bartoli, C., M. Civatte, J. F. Pellissier, and D. Figarella-Branger. 2001. CCR2A and CCR2B, the two isoforms of the monocyte chemoattractant protein-1 receptor are up-regulated and expressed by different cell subsets in idiopathic inflammatory myopathies. *Acta Neuropathol. (Berl.)* 102: 385–392.
14. De Rossi, M., P. Bernasconi, F. Baggi, R. de Waal Malefyt, and R. Mantegazza. 2000. Cytokines and chemokines are both expressed by human myoblasts: possible relevance for the immune pathogenesis of muscle inflammation. *Int. Immunol.* 12: 1329–1335.
15. Zlotnik, A., and O. Yoshie. 2000. Chemokines: a new classification system and their role in immunity. *Immunity* 12: 121–127.
16. Yoshie, O., T. Imai, and H. Nomiyama. 2001. Chemokines in immunity. *Adv. Immunol.* 78: 57–110.
17. Bazan, J. F., K. B. Bacon, G. Hardiman, W. Wang, K. Soo, D. Rossi, D. R. Greaves, A. Zlotnik, and T. J. Schall. 1997. A new class of membrane-bound chemokine with a CX3C motif. *Nature* 385: 640–644.
18. Pan, Y., C. Lloyd, H. Zhou, S. Dolich, J. Deeds, J. A. Gonzalo, J. Vath, M. Gosselin, J. Ma, B. Dussault, et al. 1997. Neurotactin, a membrane-anchored chemokine upregulated in brain inflammation. *Nature* 387: 611–617.
19. Fraticelli, P., M. Sironi, G. Bianchi, D. D'Ambrosio, C. Albanesi, A. Stoppacciaro, M. Chieppa, P. Allavena, L. Ruco, G. Girolomoni, et al. 2001. Fractalkine (CX3CL1) as an amplification circuit of polarized Th1 responses. *J. Clin. Invest.* 107: 1173–1181.
20. Imaizumi, T., H. Yoshida, and K. Satoh. 2004. Regulation of CX3CL1/fractalkine expression in endothelial cells. *J. Atheroscler. Thromb.* 11: 15–21.
21. Fujimoto, K., T. Imaizumi, H. Yoshida, S. Takanashi, K. Okumura, and K. Satoh. 2001. Interferon-γ stimulates fractalkine expression in human bronchial epithelial cells and regulates mononuclear cell adherence. *Am. J. Respir. Cell Mol. Biol.* 25: 233–238.
22. Fong, A. M., L. A. Robinson, D. A. Steeber, T. F. Tedder, O. Yoshie, T. Imai, and D. D. Patel. 1998. Fractalkine and CX3CR1 mediate a novel mechanism of leukocyte capture, firm adhesion, and activation under physiologic flow. *J. Exp. Med.* 188: 1413–1419.
23. Umehara, H., E. T. Bloom, T. Okazaki, Y. Nagano, O. Yoshie, and T. Imai. 2004. Fractalkine in vascular biology: from basic research to clinical disease. *Arterioscler. Thromb. Vasc. Biol.* 24: 34–40.
24. Garton, K. J., P. J. Gough, C. P. Blobel, G. Murphy, D. R. Greaves, P. J. Dempsey, and E. W. Raines. 2001. Tumor necrosis factor-α-converting enzyme (ADAM17) mediates the cleavage and shedding of fractalkine (CX3CL1). *J. Biol. Chem.* 276: 37993–38001.
25. Hundhausen, C., D. Misztela, T. A. Berkhout, N. Broadway, P. Saftig, K. Reiss, D. Hartmann, F. Fahrenholz, R. Postina, V. Matthews, et al. 2003. The disintegrin-like metalloproteinase ADAM10 is involved in constitutive cleavage of CX3CL1 (fractalkine) and regulates CX3CL1-mediated cell-cell adhesion. *Blood* 102: 1186–1195.
26. Nanki, T., T. Imai, K. Nagasaka, Y. Urasaki, Y. Nonomura, K. Taniguchi, K. Hayashida, J. Hasegawa, O. Yoshie, and N. Miyasaka. 2002. Migration of CX3CR1-positive T cells producing type 1 cytokines and cytotoxic molecules into the synovium of patients with rheumatoid arthritis. *Arthritis Rheum.* 46: 2878–2883.
27. Nishimura, M., H. Umehara, T. Nakayama, O. Yoneda, K. Hieshima, M. Kakizaki, N. Dohmae, O. Yoshie, and T. Imai. 2002. Dual functions of fractalkine/CX3C ligand 1 in trafficking of perforin$^+$/granzyme B$^+$ cytotoxic effector lymphocytes that are defined by CX3CR1 expression. *J. Immunol.* 168: 6173–6180.
28. Imai, T., K. Hieshima, C. Haskell, M. Baba, M. Nagira, M. Nishimura, M. Kakizaki, S. Takagi, H. Nomiyama, T. J. Schall, et al. 1997. Identification and molecular characterization of fractalkine receptor CX3CR1, which mediates both leukocyte migration and adhesion. *Cell* 91: 521–530.
29. Combadiere, C., K. Salzwedel, E. D. Smith, H. L. Tiffany, E. A. Berger, and P. M. Murphy. 1998. Identification of CX3CR1: a chemotactic receptor for the human CX3C chemokine fractalkine and a fusion coreceptor for HIV-1. *J. Biol. Chem.* 273: 23799–23804.
30. Nanki, T., Y. Urasaki, T. Imai, M. Nishimura, K. Muramoto, T. Kubota, and N. Miyasaka. 2004. Inhibition of fractalkine ameliorates murine collagen-induced arthritis. *J. Immunol.* 173: 7010–7016.
31. Kojima, T., N. Tanuma, Y. Aikawa, T. Shin, A. Sasaki, and Y. Matsumoto. 1997. Myosin-induced autoimmune polymyositis in the rat. *J. Neurol. Sci.* 151: 141–148.
32. Livak, K. J., and T. D. Schmittgen. 2001. Analysis of relative gene expression data using real-time quantitative PCR and the 2(-DDC(T)) method. *Methods* 25: 402–408.
33. Gutala, R. V., and P. H. Reddy. 2004. The use of real-time PCR analysis in a gene expression study of Alzheimer's disease post-mortem brains. *J. Neurosci. Methods* 132: 101–107.
34. Dalakas, M. C. 2002. Muscle biopsy findings in inflammatory myopathies. *Rheum. Dis. Clin. North Am.* 28: 779–798.
35. Dalakas, M. C., and R. Hohlfeld. 2003. Polymyositis and dermatomyositis. *Lancet* 362: 971–982.
36. Ito, T., T. Kumamoto, H. Horinouchi, K. Yukishige, R. Sugihara, S. Fujimoto, and T. Tsuda. 2002. Adhesion molecule expression in experimental myositis. *Muscle Nerve* 25: 409–418.
37. Matsubara, S., T. Kitaguchi, A. Kawata, K. Miyamoto, H. Yagi, and S. Hirai. 2001. Experimental allergic myositis in SJL/J mouse: reappraisal of immune reaction based on changes after single immunization. *J. Neuroimmunol.* 119: 223–230.
38. Nemoto, H., K. Nemoto, H. Sugimoto, and M. Kinoshita. 2001. FK506 suppressed the inflammatory change of EAM in SJL/J mice. *J. Neurol. Sci.* 193: 7–11.

39. Rosenberg, N. L., S. P. Ringel, and B. L. Kotzin. 1987. Experimental autoimmune myositis in SJL/J mice. *Clin. Exp. Immunol.* 68: 117–129.
40. Matsubara, S., T. Shima, and M. Takamori. 1993. Experimental allergic myositis in SJL/J mice immunized with rabbit myosin B fraction: immunohistochemical analysis and transfer. *Acta Neuropathol. (Berl.)* 85: 138–144.
41. De Bleecker, J. L., V. I. Meire, W. Declercq, and E. H. Van Aken. 1999. Immunolocalization of tumor necrosis factor-α and its receptors in inflammatory myopathies. *Neuromuscul. Disord.* 9: 239–246.
42. Kalovidouris, A. E., and Z. Plotkin. 1995. Synergistic cytotoxic effect of interferon-γ and tumor necrosis factor-α on cultured human muscle cells. *J. Rheumatol.* 22: 1698–1703.
43. Shelton, G. D., N. A. Calcutt, R. S. Garrett, D. Gu, N. Sarvetnick, W. M. Campana, and H. C. Powell. 1999. Necrotizing myopathy induced by overexpression of interferon-γ in transgenic mice. *Muscle Nerve* 22: 156–165.
44. Kuru, S., A. Inukai, Y. Liang, M. Doyu, A. Takano, and G. Sobue. 2000. Tumor necrosis factor-α expression in muscles of polymyositis and dermatomyositis. *Acta Neuropathol. (Berl.)* 99: 585–588.
45. Sawai, H., Y. W. Park, J. Roberson, T. Imai, J. J. Goronzy, and C. M. Weyand. 2005. T cell costimulation by fractalkine-expressing synoviocytes in rheumatoid arthritis. *Arthritis Rheum.* 52: 1392–1401.
46. Ancuta, P., R. Rao, A. Moses, A. Mehle, S. K. Shaw, F. W. Luscinskas, and D. Gabuzda. 2003. Fractalkine preferentially mediates arrest and migration of $CD16^+$ monocytes. *J. Exp. Med.* 197: 1701–1707.
47. Thieblemont, N., L. Weiss, H. M. Sadeghi, C. Estcourt, and N. Haeffner-Cavaillon. 1995. $CD14^{low}CD16^{high}$: a cytokine-producing monocyte subset which expands during human immunodeficiency virus infection. *Eur. J. Immunol.* 25: 3418–3424.
48. Belge, K. U., F. Dayyani, A. Horelt, M. Siedlar, M. Frankenberger, B. Frankenberger, T. Espevik, and L. Ziegler-Heitbrock. 2002. The proinflammatory $CD14^+CD16^+DR^{++}$ monocytes are a major source of TNF. *J. Immunol.* 168: 3536–3542.
49. Feng, L., S. Chen, G. E. Garcia, Y. Xia, M. A. Siani, P. Botti, C. B. Wilson, J. K. Harrison, and K. B. Bacon. 1999. Prevention of crescentic glomerulonephritis by immunoneutralization of the fractalkine receptor CX3CR1 rapid communication. *Kidney Int.* 56: 612–620.
50. Lesnik, P., C. A. Haskell, and I. F. Charo. 2003. Decreased atherosclerosis in $CX3CR1^{-/-}$ mice reveals a role for fractalkine in atherogenesis. *J. Clin. Invest.* 111: 333–340.
51. Combadiere, C., S. Potteaux, J. L. Gao, B. Esposito, S. Casanova, E. J. Lee, P. Debre, A. Tedgui, P. M. Murphy, and Z. Mallat. 2003. Decreased atherosclerotic lesion formation in CX3CR1/apolipoprotein E double knockout mice. *Circulation* 107: 1009–1016.

■ 免疫学的検査/自己免疫関連検査

抗Sm抗体

上阪　等

異常値の出るメカニズムと臨床的意義

抗Sm抗体は全身性エリテマトーデス(SLE)患者の血清に見いだされて報告された自己抗体で，発見の由来となった患者名Smithの初めの2文字が冠されている．以前よく用いられた受身血球凝集(PHA)法による抗ENA抗体測定でRNase抵抗性抗体として検出される 抗核抗体(anti-nuclear antibody：ANA)の1つである．

この抗体は，細胞核内のRNA/リボ核蛋白複合体である核内低分子リボ核蛋白(small nuclear ribonucleoprotein：sn-RNP)分子のうちのU1，U2，U4/6，U5RNPと反応する．抗体結合蛋白はこれらの蛋白の共通構成成分であるB/B'，D1，D2，D3，E，F，Gなどの蛋白である．なかでもB/B'，D1，D3が認識されていることが多く，E，F，G蛋白はnativeな形でのみ認識される．

そもそもリボ 核蛋白は核内でRNAの成熟に関与する重要な蛋白である．しかし，この抗体をもつ患者の臨床症状がリボ核蛋白機能の障害に基づくわけではない．代わりに，この抗体はSLE診断の補助としての重要な臨床的意義をもつ．

この自己抗体が産生されるメカニズムは不明であるが，D蛋白とEpstein-Barr(EB)ウイルスのEBNA蛋白に分子上の相同性が認められるため，EBウイルス感染が契機であるとするものもいる．

臨床上の重要性と選択

●代表的なANAであり，原則として蛍光抗体法によるANA陽性例にのみ見いだされる．斑紋型(speckled pattern)に核が染色される例が多い．

● SLE患者に特異性が高く見いだされ，アメリカリウマチ学会によるSLEの分類基準にも組み入れられている．

● SLEの症状の中では腎症状，中枢神経症状の重症度との関連も報告されたが，これを否定する報告もあり，決定的なものはない．

●一方で，疾患活動性の高い症例で陽性になることが多く，そのために，疾患活動性が高いことにより，自己抗体が多クローン性に産生される状態で陽性になるという解釈がある．

正常と異常の判断

二重免疫拡散(DID)法では陰性．ELISA法では7.0 index未満(判定保留7.0～30.0 index)，陽性30.0 index以上．ELISA法にも種々の方法があり，一概にいえないものの，二重免疫拡散法より感度に勝るが，特異度に劣ると考えられている．

RNase抵抗性ENA抗体としては，PHA法で40倍以下である．

●生理的変動はない．

異常を示す疾患・病態

SLE患者の15～30%ほどに陽性とされる．陽性率には人種差が認められ，アフリカ系アメリカ人に多い．疾患特異性は極めて高く，他に陽性となるのはSLEの病態を包含する混合性結合織病やオーバーラップ症候群(10～20%程度)である．稀にSjögren症候群や強皮症などその他の膠原

こうさか ひとし：東京医科歯科大学大学院医歯学総合研究科膠原病・リウマチ内科　〒113-8519 東京都文京区湯島1-5-45

病や未分類膠原病でも陽性になることもある．

SLEでこの抗体が陽性の場合は，疾患活動性が高いことが多く，陰性となるまで月1度程度のフォローアップが望まれる．

関連検査

抗γ-グロブリン血症を持つ症例では，ELISA法で境界値ないし弱陽性を呈することがある．この際にはDID法で確認する必要がある．また，ほとんどの抗Sm抗体陽性血清は抗U1RNP抗体をもつ．初めにSm抗体が陽性になり，SLEの経過とともに抗U1RNP抗体が陽性となる例もあるものの，基本的に抗U1RNP抗体陰性例では抗Sm抗体陽性の判定に慎重であるべきである．

真の抗Sm抗体陽性例ではSLEを疑い，検査として抗DNA抗体，血清補体価，免疫複合体などの測定を行うべきである．

検査費用と保険請求

保険適用あり(保険点数は免疫拡散法，ELISA法ともに190点)．

文献
1) Migliorini P, et al：Anti-Sm and anti-RNP antibodies. Autoimmunity 38：47-54, 2005

抗 Scl-70 抗体

上阪　等

異常値の出るメカニズムと臨床的意義

抗 Scl-70 抗体は強皮症(scleroderma)に特異的に出現するとして報告された自己抗体である．Scl は sclerodema の略で，70 は抗体の反応する抗原の分子量が 70 kDa であったことに由来する．同じ抗体は，Og 抗体など他の名称でも呼ばれた．その後，対応抗原が細胞核内に存在する DNA トポイソメラーゼ I であることが明らかになり，さらに分子量も実際は 100 kDa で，当初報告された 70 kDa 蛋白はトポイソメラーゼ I が部分分解されたものであったことがわかり，近年は抗トポイソメラーゼ I 抗体と呼ばれることもある．

トポイソメラーゼ I は二本鎖 DNA の超らせん構造を巻き戻す酵素の 1 つで，遺伝子発現や複製といった細胞の基本機能にかかわる酵素である．血清中に検出される本抗体が，細胞核内のかかる酵素を抑制して症状を起こす可能性はまず考えられない．この抗体も，他の自己抗体の多くと同様に，産生メカニズムは不明である．しかしながら，強皮症の診断や予後の推定に役立つ重要な自己抗体である．

臨床上の重要性と選択

●代表的な抗核抗体(anti-nuclear antibody：ANA)であり，蛍光抗体法による ANA 陽性例にのみ見いだされる．蛍光抗体法では，均質型(homogenous pattern)に近い斑紋型(speckled pattern)を呈することが多い．

●強皮症に特異性が極めて高く，他の膠原病や強皮症患者近親の健常者でも陽性になることはまずないと考えてよい．

●ことに皮膚硬化が肘を越えた近位部にも拡がるびまん性皮膚硬化型の強皮症に高頻度に認められ，進行性の肺線維症などの内臓病変を合併する頻度も高いとされる．

正常と異常の判断

二重免疫拡散(DID)法では陰性．ELISA 法では 16.0 index 未満(判定保留 16.0～24.0 index)，陽性，24.0 index 以上

ELISA 法は，従来，DID 法より感度に劣るとされてきたが，改良が進んでいる．ただし，ELISA 法の特異度は低いことが多く，方法によっては全身性エリテマトーデス(SLE)症例の 25%や C 型ウイルス肝炎患者で陽性だったとする報告もある．したがって，ELISA 法で低力価陽性の場合には解釈に注意を要する．

●生理的変動についての報告はない．

異常を示す疾患・病態

強皮症患者全体の 20～40%程度に陽性であるが，びまん性皮膚硬化型に限れば 40～50%に達し，限局型では 10 %程度である．その反面，他の疾患ではほとんど陰性である．病初限局型の皮膚硬化を持つ症例でも，本抗体陽性者の場合には長期的には皮膚硬化範囲が拡大しやすい．

抗 Scl-70 抗体陽性の強皮症例では，肺線維症が重症化しやすいとされる．肺線維化を伴う症例の半分程度までが本抗体陽性ともいわれ，また本抗体陽性例は肺機能の長期予後が悪いという．た

こうさか ひとし：東京医科歯科大学大学院医歯学総合研究科膠原病・リウマチ内科　〒113-8519 東京都文京区湯島 1-5-45

だし，最近のメタ解析では，本抗体と肺線維化の関連は従来ほど高くはないとの結果もある．

また，本抗体陽性例は陰性例に比べて死亡率が高く，おそらく肺疾患が原因となった心不全が多いことを反映していると考えられている．一方，腎クリーゼ発症や癌合併との関連を報告したものもあるが，これらを確認できた報告はない．

稀に，特発性間質性肺炎や逆流性食道炎とされている症例に，抗 Scl-70 抗体を認めることがある．これらの症例も経過を追うと皮膚硬化が現れることが多く，内臓病変の先行した強皮症ととらえられる．また，Raynaud 現象のみを症状とする患者も，本抗体陽性例では将来的に強皮症を発症する危険性が高い．

なお，皮膚硬化や肺線維化の軽い強皮症症例で，経過とともに抗 Scl-70 抗体が陰性化したという報告もあるが，患者の大多数は，診断時に陽性であれば，経過を通じて陽性であり，また陰性例が陽性化することもほとんどない．さらに，抗体価が疾患活動性を反映することもない．したがって，定期的にフォローアップすべき抗体ではない．

関連検査

同じく強皮症患者に見いだされる抗セントロメア抗体は，CREST 症候群など限局皮膚硬化型の症例に陽性になることが多い．この抗体は，蛍光抗体法では特徴的な散在斑点型(discrete speckled pattern)を呈する ANA として検出される．

ただし，抗セントロメア抗体が抗 Scl-70 抗体と共存することは稀で，抗 Scl-70 抗体陽性例のうちの 0.5%しか抗セントロメア抗体を持っていなかったという統計もある．

検査費用と保険請求

保険適用あり(保険点数は免疫拡散法，ELISA 法ともに 170 点)．

文献

1) Basu D, et al : Anti-Scl-70.. Autoimmunity 38 : 65-72, 2005

ARTHRITIS & RHEUMATISM2
Vol. 54, No. 7, July 2006, pp 2074–2083
DOI 10.1002/art.21927

Direct Modulation of Rheumatoid Inflammatory Mediator Expression in Retinoblastoma Protein–Dependent and –Independent Pathways by Cyclin-Dependent Kinase 4/6

Yoshinori Nonomura,[1] Kenji Nagasaka,[2] Hiroyuki Hagiyama,[2] Chiyoko Sekine,[1] Toshihiro Nanki,[2] Mimi Tamamori-Adachi,[2] Nobuyuki Miyasaka,[2] and Hitoshi Kohsaka[1]

Objective. **It is known that the cyclin-dependent kinase inhibitor (CDKI) gene $p21^{Cip1}$ suppresses rheumatoid inflammation by down-modulating type I interleukin-1 receptor (IL-1RI) expression and inhibiting JNK activity. The purpose of this study was to determine whether CDK activity directly modulates the production of inflammatory molecules in patients with rheumatoid arthritis (RA).**

Methods. **Genes for the CDKIs $p16^{INK4a}$ and $p18^{INK4c}$, a constitutively active form of retinoblastoma (RB) gene product, cyclin D1, and CDK-4, were transferred into RA synovial fibroblasts (RASFs). RASFs were also treated with a synthetic CDK-4/6 inhibitor (CDK4I). Levels of matrix metalloproteinase 3 (MMP-3), monocyte chemoattractant protein 1 (MCP-1), and IL-1RI expression were determined by Northern blotting, real-time polymerase chain reaction analysis, and enzyme-linked immunosorbent assay. CDKIs were immunoprecipitated to reveal their association with JNK.**

Results. **Transfer of the $p16^{INK4a}$ and $p18^{INK4c}$ genes and CDK4I suppressed the production of MMP-3 and MCP-1. Unlike $p21^{Cip1}$, neither CDKI gene inhibited IL-1RI or JNK. The expression of MMP-3 was up-regulated when CDK-4 activity was augmented. This regulation functioned at the messenger RNA (mRNA) level in MMP-3, but not in MCP-1. Transfer of active RB suppressed the production of MMP-3 and MCP-1 without changing their mRNA levels.**

Conclusion. **CDK-4/6 modulated the production of MMP-3 and MCP-1. MMP-3 production was regulated primarily at the mRNA level in an RB-independent manner, whereas MCP-1 production was controlled posttranscriptionally by RB. These results show that cell cycle proteins are associated with control of mediators of inflammation through multiple pathways.**

Rheumatoid arthritis (RA) is a chronic inflammatory disease characterized by synovial inflammation, hyperplasia, and destruction of the cartilage and bone. In the rheumatoid joint, inflammatory cells, such as lymphocytes and macrophages, infiltrate and produce a variety of cytokines. The inflammatory cells stimulate synovial fibroblasts to proliferate vigorously and to secrete inflammatory cytokines, and they also recruit more inflammatory cells into affected joints. Proliferating RA synovial fibroblasts (RASFs) and infiltrating cells shape a hyperplastic granulomatous synovial tissue called pannus. Pannus offers a platform where many mediators of inflammation, including tissue-degrading proteases, are produced and osteoclasts are activated to absorb the bone matrix. These processes eventually lead to destruction of the affected joints (1,2).

A goal of antirheumatic treatment is prevention of irreversible joint damage. Clinical experience with

Supported by grants from the Ministry of Health, Labor, and Welfare of Japan, the Ministry of Education, Culture, Sports, Science, and Technology of Japan, and the Kato Memorial Bioscience Foundation.

[1]Yoshinori Nonomura, MD, PhD, Chiyoko Sekine, PhD, Hitoshi Kohsaka, MD, PhD: Tokyo Medical and Dental University, Tokyo, and RIKEN Research Center of Allergy and Immunology, Yokohama, Japan; [2]Kenji Nagasaka, MD, PhD, Hiroyuki Hagiyama, MD, PhD, Toshihiro Nanki, MD, PhD, Mimi Tamamori-Adachi, MD, PhD, Nobuyuki Miyasaka, MD, PhD: Tokyo Medical and Dental University, Tokyo, Japan.

Drs. Nonomura and Nagasaka contributed equally to this work.

Address correspondence and reprint requests to Hitoshi Kohsaka, MD, PhD, Department of Medicine and Rheumatology, Graduate School, Tokyo Medical and Dental University, 1-5-45, Yushima, Bunkyo-ku, 113-8519 Tokyo, Japan. E-mail: kohsaka.rheu@tmd.ac.jp.

Submitted for publication August 1, 2005; accepted in revised form March 20, 2006.

blockage of inflammatory cytokines, such as tumor necrosis factor α (TNFα), interleukin-1β (IL-1β), and IL-6, has demonstrated that antiinflammatory cytokine treatment is an attractive therapeutic choice for RA (3). Nevertheless, the effects of such new antiinflammatory treatment as well as conventional treatment are never satisfactory for all RA patients. We have been exploring cell cycle regulation of RASFs as a new antirheumatic strategy, assuming that suppression of inflammation, together with synovial cell proliferation, should be the ultimate therapeutic combination. The efficacy of cell cycle regulation was substantiated previously by transfer of cyclin-dependent kinase inhibitor (CDKI) genes $p16^{INK4a}$ and $p21^{Cip1}$ into inflamed joints in animal models of RA (4–6).

In general, the cell cycle is driven by kinase activity of cyclin–CDK complexes. These kinases phosphorylate retinoblastoma (RB) gene products, which results in inactivation of the RB function that keeps E2F transcription factors from promoting cell cycle progression. CDKIs are intracellular proteins that inhibit the kinase activity of CDKs. They consist of 2 families, INK4 and Cip/Kip. The INK4 family proteins, including $p15^{INK4b}$, $p16^{INK4a}$, $p18^{INK4c}$, and $p19^{INK4d}$, specifically inhibit the cyclin D–CDK-4/6 complex, which is important for the G_1/S transition of the cell cycle. The Cip/Kip family proteins, including $p21^{Cip1}$, $p27^{Kip1}$, and $p57^{Kip2}$, inhibit all cyclin–CDK complexes (7).

While CDKIs act as inhibitors of cell cycling, we have observed that CDKI gene delivery into arthritic joints suppresses not only the proliferation of synovial fibroblasts, but also the production of inflammatory cytokines, infiltration by inflammatory cells, and destruction of bone and cartilage (5). We have also found that expression of $p21^{Cip1}$ in RASFs in vitro down-regulates the messenger RNA (mRNA) expression of proteinases and mediators of inflammation involved in the pathology of RA (8). These observations are consistent with reports showing that $p21^{Cip1}$ binds to JNK to exert antiinflammatory effects (9,10). In addition, we have found that expression of IL-1 receptor type I (IL-1RI) is down-regulated and that transcription factor activities, including NF-κB and activator protein 1 (AP-1), are suppressed by $p21^{Cip1}$ (8).

In contrast, we identified no mechanistic interaction between $p16^{INK4a}$ and other molecules in RASFs (8). Nevertheless, some inflammatory molecules, including matrix metalloproteinase 3 (MMP-3) and monocyte chemoattractant protein 1 (MCP-1), were down-regulated, commonly by $p16^{INK4a}$ and $p21^{Cip1}$ (8). This led us to assume that CDK activity directly modulates the expression of inflammatory molecules. The findings of the present study have shown that this is indeed the case, at least in terms of MMP-3 and MCP-1 production. Their protein levels were regulated by RB-dependent as well as RB-independent pathways. We found that cell cycle progression and inflammatory processes in arthritic joints are closely related.

MATERIALS AND METHODS

Cell culture. RA synovial tissues were obtained from 5 patients who had undergone joint replacement surgery or synovectomy at Tokyo Medical and Dental University Hospital, Tokyo Metropolitan Bokuto Hospital, or National Shimoshizu Hospital in Chiba. All patients fulfilled the American College of Rheumatology (formerly, the American Rheumatism Association) criteria for the classification of RA (11). The mean ± SD duration of disease was 10.6 ± 3.9 years. At the time samples were collected, the patients had been taking disease-modifying antirheumatic drugs (DMARDs) (methotrexate, gold sodium thiomalate, bucillamine, or sulfasalazine) with or without prednisolone. The RA was refractory to these medications. The mean ± SD erythrocyte sedimentation rate was 53 ± 27.0 mm/hour before surgery.

Synovial tissue was also obtained from a patient with osteoarthritis (OA). Adult normal human dermal fibroblasts (NHDF-Ad) derived from 1 subject were purchased from Cambrex (East Rutherford, NJ). RASFs and OA synovial fibroblasts (OASFs) were isolated and cultured as described elsewhere (4). All fibroblast samples were used at early passages (from passage 3 to 9).

Patients gave their consent to all procedures in the present study. The study protocol was approved by the ethics committees of Tokyo Medical and Dental University and of RIKEN.

Adenovirus infection. Recombinant adenoviruses containing a human $p16^{INK4a}$ gene (AxCAp16) (12), a human $p18^{INK4c}$ gene (Ad-RGD-p18) (13–15), a human $p21^{Cip1}$ gene (AxCAp21) (12), a human cyclin D1 in conjunction with a nuclear localization signal (Ad-D1-NLS) and a human CDK-4 gene (Ad-CDK-4) (16,17) that encodes a nonphosphorylatable, constitutively active form of a human RB gene (Ad-RB) or a β-galactosidase gene (Ad-LacZ) (18,19), control Ax1w1 adenovirus (RIKEN Gene Bank, Tsukuba, Japan), and control Ad5-RGD, which lacks insert genes (20), were either purchased, received as gifts, or constructed in our laboratory. RASFs, OASFs, and NHDF-Ad were infected with one of these recombinant adenoviruses at a minimal multiplicity of infection (MOI) that ensured 100% efficacy of infection (typically, 50–200 MOI).

Three days after infection, when expression of the transferred genes reached maximal levels, the fibroblasts were examined for proliferation or were stimulated for 5 hours with 5 ng/ml of TNFα (Genzyme, Cambridge, MA), 5 ng/ml of IL-1β (PeproTech, Rocky Hill, NJ), and 25 μM indomethacin (Sigma, St. Louis, MO) to examine the production of mediators of inflammation. Indomethacin was included to avoid possible suppression by prostaglandins released from the stimulated RASFs (8,21). Preliminary experiments had shown that